BENCHMARKING OF THE MULTIGROUP, FINE MESH, SP_3 METHODS IN PARCS WITH THE VENUS-2 MOX CRITICAL EXPERIMENTS

Tomasz Kozlowski Chang-Ho Lee Thomas J. Downar
Purdue University
School of Nuclear Engineering
1290 Nuclear Engineering Building
West Lafayette, Indiana 47907-1290
United States
tomasz@ecn.purdue.edu changho@ecn.purdue.edu downar@ecn.purdue.edu

ABSTRACT

A multigroup, pin-by-pin, transport capability has been added to the U.S. NRC neutron kinetics code PARCS for the purpose of analyzing MOX fueled cores. The focus of the work reported here is the benchmarking of the new PARCS methods using the VENUS-2 critical experiments. Both the two- and three-dimensional versions of the benchmark were analyzed with PARCS using group constants generated with the HELIOS lattice physics code. The 2-D VENUS-2 benchmark was performed with a specified axial buckling and PARCS results are compared to a full core transport solution generated with HELIOS. The 3-D VENUS-2 benchmark is still a "blind" benchmark and assembly and axial power distributions from PARCS results are reported. The PARCS core calculation was performed using a fine mesh SP_3 kernel with 2 and 8 energy groups with cell homogenized cross sections. A conventional 2 group nodal calculation with pin power reconstruction was performed using PARCS ANM kernel in order to compare the new methods in PARCS with conventional core analysis methods. A preliminary analysis was also performed using SPH factors to account for errors introduced by pin cell homogenization.

1. INTRODUCTION

This past year a multigroup, pin-by-pin, transport capability was added to the U.S. NRC neutron kinetics code PARCS for the purpose of analyzing MOX fueled cores [1, 2]. In order to assess the new methods, the OECD/NEA VENUS-2 MOX benchmark was performed with PARCS. VENUS-2 is an international benchmark with both two- and three-dimensional exercises [3, 4]. The VENUS facility is a zero power critical reactor located at SCK CEN in Belgium. The core consists of 12 15x15 assemblies with the typical pitch of 17x17 assembly, 1.26 cm. The four central assemblies consist of the 3.3 w/o UO_2 fuel pins, with 10 Pyrex pins each. The 8 assemblies on the periphery of the core consist of UO_2 and MOX fuel: 7 internal rows contain 4.0 w/o UO_2 fuel pins, 8 external rows contain MOX fuel with 2.0/2.7 w/o high-grade plutonium. The core is 50 cm in height.

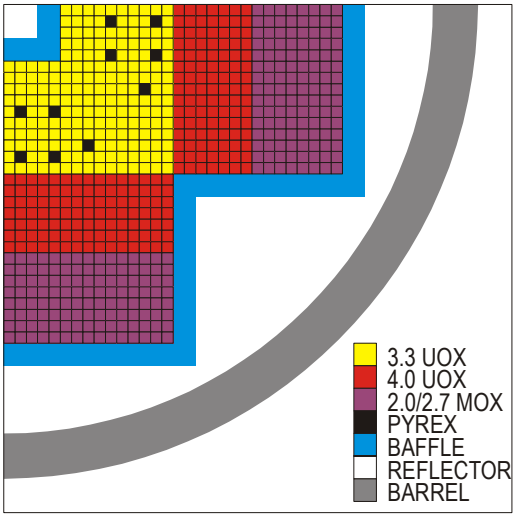

Figure 1. VENUS-2 1/4 core geometry.

The 2-D VENUS-2 experimental data consists of pin power distribution measurements in 121 of the 325 fuel rods in 1/8th of the core: 41 with 3.3 w/o UO2, 35 with 4.0 w/o and 45 with 2.0/2.7 w/o MOX. The remainder of the pin powers were interpolated from the measured values. The 3-D VENUS-2 experimental data provides radial pin power measurement and axial fission power of six selected pins.

A complete description of the facility is given in the benchmark specifications, which includes all geometry and material composition data required to create a detailed computational model of the VENUS-2 core. The objective of the benchmark was to validate and compare the nuclear data sets and production codes used for MOX-fuelled system calculations. The comparison with experimental data facilitates identifying the source of discrepancies between calculations and measurements and to quantify the relative merits of the different calculation methods.

2. HELIOS MODEL AND RESULTS FOR THE VENUS-2 BENCHMARK

The reference solution in the work here was generated using the HELIOS 1.7 lattice code [5]. HELIOS employs the Current Coupling Collision Probability (CCCP) method and is capable of modeling generalized 2-D geometries. A detailed HELIOS model was constructed for VENUS-2 using the 8-sector "windmill" mesh in the coolant of each pin cell. This mesh divides the sides of a cell into three flat-current segments, thus accurately modeling the dip in the thermal currents caused by the fuel in the middle of each side of the pin. A square mesh the size of the pin pitch was used to discretize the baffle and reflector regions. For the reference calculation, a 190 energy group neutron library was used and the current coupling parameter k=4 was applied as recommended by the HELIOS manual. The axial buckling specified in the benchmark of 2.39×10^{-3} cm^2 was used throughout the core region. Because the core was symmetric, it was necessary to model only 1/8th of the core.

Because one of the objectives here was to use HELIOS to benchmark PARCS, a modeling simplification was made to allow a consistent comparison between HELIOS and PARCS solutions. The core barrel and all other external structure material was neglected and replaced by the reflector. This was done in order to simplify the generation of homogenized cross sections for PARCS. The difference in eigenvalue of the HELIOS model with and without core barrel was only about 20 pcm.

The 2-D version of the benchmark consists of both pin cell and core calculations. Table I shows the pin cell k_{inf} results for the other benchmark participants who also used the HELIOS code. The results percent deviations are relative to all other benchmark participants. As indicated, there is good agreement in the results, particularly for the two HELIOS solutions that used the 190 group library.

Table I. HELIOS results for VENUS-2 pin cells.

Institution	**Code**	**UO_2 3.3%**		**UO_2 4.0%**		**MOX**	
		k_{inf}	**%Dev.***	**k_{inf}**	**%Dev.**	**k_{inf}**	**%Dev.**
ORNL	HELIOS 1.4 (190g)	1.40847	0.18	1.34333	0.45	1.26254	0.46
KAERI	HELIOS 1.5 (35g)	1.40904	0.22	1.34306	0.43	1.26339	0.53
Purdue	HELIOS 1.7 (190g)	1.40850	0.18	1.34331	0.45	1.26339	0.53
Average**		1.40593		1.33726		1.25673	

*Deviation from the average k_{inf}

**Average k_{inf} of all benchmark participants

The core eigenvalue and pin power predictions of the same three HELIOS solutions is shown in Table II and compared to experimental values. Again, there is good agreement in the results, particularly for the two 190 group results.

Table II. HELIOS results for the 2-D VENUS-2 benchmark.

Institution	**Code**	**Core k-eff**	**Pin Type % RMS**			
			UO_2 3.3%	**UO_2 4.0%**	**MOX**	**All**
ORNL	HELIOS 1.4 (190g)	0.99870	1.57	2.08	3.25	2.45
KAERI	HELIOS 1.5 (35g)	0.99817	2.51	1.54	5.02	3.49
Purdue	HELIOS 1.7 (190g)	0.99749	1.65	1.86	3.29	2.44

3. PARCS MODEL OF THE VENUS-2 CORE

A VENUS-2 model was then constructed using the U.S. NRC core simulator PARCS v2.1. A solution was performed using the recently developed pin-by-pin multigroup SP_3 capability, as well as with the conventional 2 group ANM nodal calculation with pin power reconstruction. This provided the ability to assess a wide range of the space, energy, angle and homogenization approximations used in solving the VENUS-2 problem.

Two sets of 2 and 8 group pin cell cross sections were generated using the HELIOS VENUS-2 model described above. The fuel and radial reflector cross sections were generated based on three single assembly calculations: two for different fuel assemblies and one two-node fuel-reflector calculation. The assembly configuration used for each calculation and the summary of parameters generated is shown in Table III.

Table III. HELIOS calculation models for generating PARCS cross sections.

Single Assembly Calculation	**Nodal Parameters Generated**	**Fine Mesh Parameters Generated**
3.3% UOX assembly 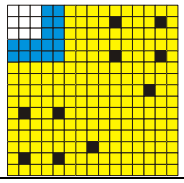	1. 2G assembly XS 2. 2G pin power form functions 3. ADFs/CDFs	2 and 8G average cell XS: 1. 3.3% UOX 2. Pyrex 3. Inner baffle 4. Inner reflector
4.0% UOX/MOX assembly 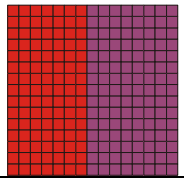	4. 2G assembly XS 5. 2G pin power form functions 6. ADFs/CDFs	2 and 8G average cell XS: 5. 4.0% UOX 6. 2.0/2.7% MOX
Fuel-Reflector assembly 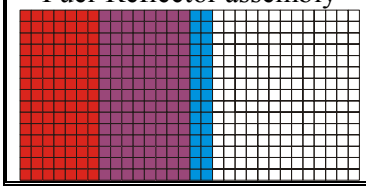	7. 2G reflector XS 8. ADFs	2 and 8G average cell XS: 7. Outer baffle 8. Outer reflector

The Assembly Discontinuity Factors (ADF) for reflector assemblies were calculated by solving analytically the 1-D diffusion equation in the homogeneous reflector region with the fuel-reflector boundary condition from HELIOS. An additional cross section set was not generated for the corner reflector with baffle on two sides. Instead, the scattering cross section was modified using the following equation [6]:

$$r = \frac{FA\ Pitch - Baffle\ Thickness}{FA\ Pitch} \tag{1}$$

The axial reflector cross sections for the 3-D version of the VENUS-2 benchmark were based on the homogeneous fuel-heterogeneous reflector model. The entire axial reflector region was collapsed into a single cross section set for each fuel type and was used in both the nodal and fine mesh calculations. A schematic of the axial reflector configuration is shown in Figure 2.

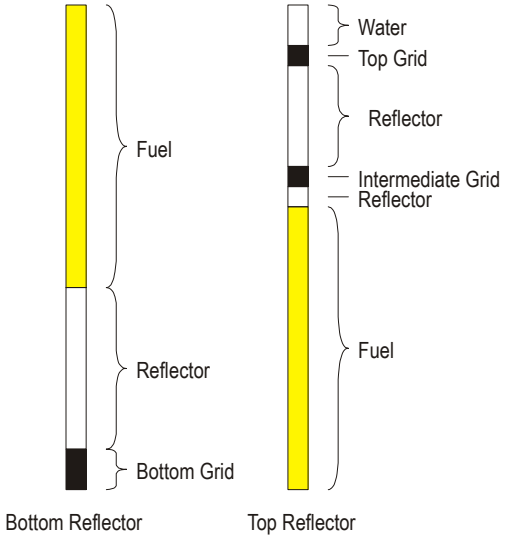

Figure 2. Schematic of the axial reflector configuration.

4. PARCS RESULTS FOR THE VENUS-2 BENCHMARK

The PARCS solutions to the 2-D VENUS-2 benchmark are summarized in Table IV. The errors are relative to the HELIOS solution shown previously in Table II. The lowest order 2 group nodal diffusion calculation predicts the eigenvalue very well but shows large errors in the pin power prediction. Of particular significance is the error in the prediction of the pin powers in the MOX assembly which shows an RMS value over 8% and a maximum pin error of 18.8%. This is most likely because of the severe flux spectral mismatch at the core / reflector interface where the MOX assemblies are located. A 2 group calculation is unable to model accurately neutron transport in this region where the flux is changing rapidly. The large error in the 3.3 w/o UO_2 assembly is probably not as significant since it is most likely the result of difficulties homogenizing the fuel assembly with water hole region and consequently difficulties obtaining accurate corner discontinuity factors for the flux reconstruction.

The pin power error is reduced significantly with the fine mesh, 8 group diffusion calculation. The RMS and maximum error values are reduced by more than 50% compared to the 2 group fine mesh solution. However, there was not much change in the results when the fine mesh 8 group solution was performed using the SP_3 approximation, which implies this problem does not contain strong transport effects.

Table IV. PARCS 2-D VENUS-2 results compared to HELIOS.

Method	Group	Angle	Core k_{eff}	Pin Type %RMS max % error (peak pin % error)			
				UO_2 3.3	UO_2 4.0	MOX	All
Nodal	2	Diffusion	0.99990	7.26 -13.3 (-9.6)	4.86 10.3 (0.4)	8.02 18.8 (3.6)	6.90 18.7 (0.4)
Fine Mesh*	2	Diffusion	0.99727	3.50 -6.2 (-2.4)	1.71 -3.9 (-3.9)	5.96 8.7 (1.8)	4.22 8.7 (-3.9)
		SP_3	1.00486	3.24 -5.7 (-2.2)	2.00 -4.5 (-4.5)	6.09 9.9 (0.6)	4.27 9.9(-4.5)
	8	Diffusion	0.99360	1.78 -3.1 (-1.0)	1.39 4.0 (-1.6)	3.22 5.6 (0.6)	2.33 5.6 (-1.6)
		SP_3	1.00284	1.80 -3.2 (-1.1)	1.55 4.4 (-2.2)	3.27 6.0 (-0.2)	2.39 6.0 (-2.2)

*4x4 mesh per pin

Since the 3-D VENUS-2 benchmark is currently "blind", the experimental results and the results of other participants are currently not available. The PARCS core k_{eff} and assembly power predictions are shown in Table V and the axial power profile is show in Figure 3.

Table V. PARCS 3-D VENUS-2 results.

Method	Group	Angle	Core k_{eff}	Assembly Power	
				Central Assembly	Peripheral Assembly
Nodal	2	Diffusion	1.00165	1.2510	0.8745
Fine Mesh*	2	Diffusion	0.99795	1.1335	0.9332
		SP_3	1.00765	1.1371	0.9314
	8	Diffusion	0.99063	1.1514	0.9243
		SP_3	1.00294	1.1520	0.9240

*4x4 mesh per pin, 1.25 cm axial mesh size

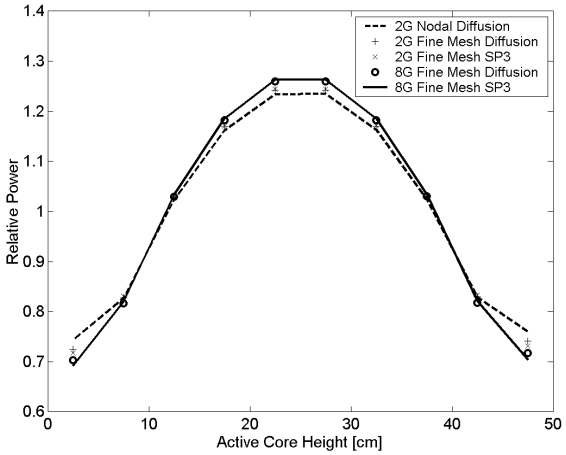

Figure 3. PARCS axial power distribution for 3-D VENUS-2.

5. THE APPLICATION OF SPH FACTORS TO VENUS-2

Although the fine-mesh core calculation treats each pin explicitly, other researchers have shown that homogenization of the pin cell can introduce significant errors into the solution [7]. As shown in Table IV, the errors in the PARCS multigroup, cell homogenized, SP_3 solution still differ by several percent and several hundred pcm from the HELIOS solution. Since explicit modeling of fuel, clad, and moderator regions is beyond the scope of PARCS capabilities, an initial effort was made to examine alternate means to recover the pin cell homogenization error without performing additional lattice calculations. A promising method for treating pin cell homogenization error is superhomogenization theory [8] and a preliminary investigation was made into the application of SPH factors to the PARCS solution of VENUS-2.

5.1 GENERATION OF SPH FACTORS

The essential idea of SPH factors is to enforce equivalence between high order and low order operators by adjusting pin homogeneous cross sections used in the low order calculation to reproduce reaction rates of the higher order calculation. In order to generate SPH factors, the only additional information necessary is the cell flux. In the work here this was edited from HELIOS from the same single assembly calculations described in Table III. A unique cell homogeneous flux was defined for each cell using flux volume weighting:

$$\phi_{I,G}^{HELIOS} = \sum_{g \in G} \sum_{i \in I} \phi_{i,g} V_i \tag{2}$$

where ϕ and V follow the standard notation for flux and volume, fine energy group g is collapsed to coarse group G and heterogeneous region i is homogenized into cell region I.

In order to preserve reaction rates between the heterogeneous HELIOS calculation and the cell homogeneous PARCS calculation, SPH factors, $\mu_{I,G}$, were introduced to correct the cell homogeneous cross sections according to the following equation:

$$\Sigma'_{I,G} = \mu_{I,G} \Sigma_{I,G} \tag{3}$$

The SPH factor $\mu_{I,G}$ was found using an iterative process. Initially, all SPH factors were initialized to be unity. At the beginning of each SPH iteration, every cross section, including the diffusion coefficient, was multiplied by the SPH factor. The PARCS solution kernel was then executed to compute a new flux with the modified cross sections. The flux is then normalized, and new SPH factors are calculated according to Eqs. 4 and 5:

$$\phi_{I,G}^{*PARCS} = \phi_{I,G}^{PARCS} \frac{\sum_I \phi_{I,G}^{HELIOS}}{\sum_I \phi_{I,G}^{PARCS}} \tag{4}$$

$$\mu_{I,G} = \frac{\phi_{I,G}^{HELIOS}}{\phi_{I,G}^{*PARCS}} \tag{5}$$

The process is repeated until a convergence tolerance of 10^{-4} was achieved for the relative infinite norm for every group.

In order to verify this method, the SPH factors were first generated using a HELIOS full core calculation. The full core HELIOS cross sections and fluxes were used to compute SPH factors which were then applied to PARCS. The resulting eigenvalue and pin power distribution of the PARCS solution reproduced exactly the HELIOS whole core solution, which essentially verified the SPH theory and the methods used to generate the SPH factors. However, it is not practical to use a whole core HELIOS solution to generate the SPH factors. Instead, it would be advantageous to generate SPH factors from the same HELIOS single fuel assembly calculations used to generate the few group cross sections for PARCS, as described in Table III.

The SPH factors were generated using HELIOS single assembly calculations for lower order PARCS calculations using 4x4 mesh per pin. The SPH factors for the 2 group diffusion solution in the 3.3% UOX assembly are shown graphically in Figure 4. The SPH factors in the fast group are relatively close to 1.0, increasing only in the central hole region and decreasing in the location of the Pyrex pins. The thermal group SPH factors vary between 1.3 and 0.7. This indicates that the cross sections must be adjusted by as much as 30% in order to reproduce HELIOS fuel assembly reaction rates.

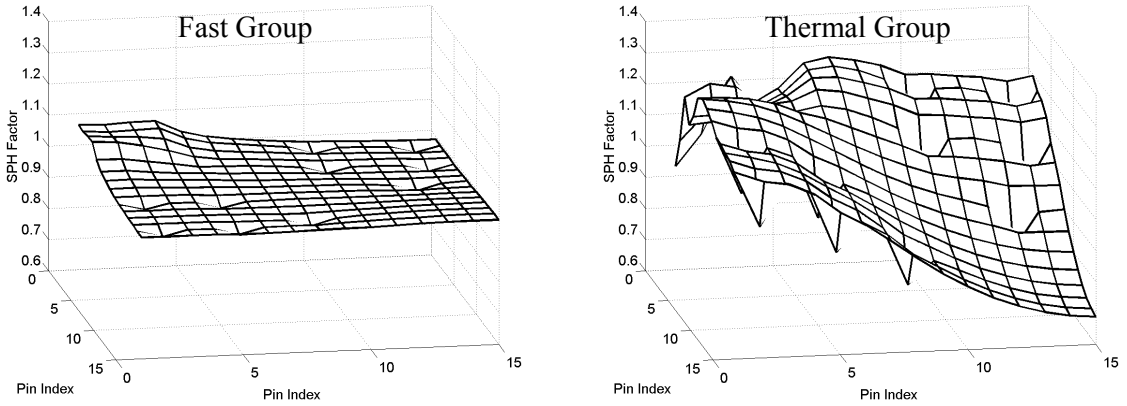

Figure 4. SPH factors for the 3.3% UOX assembly (4x4 mesh, diffusion).

5.2 VENUS-2 RESULTS WITH SPH FACTORS

The SPH factors generated with a single assembly HELIOS calculations were then applied to lower order PARCS solutions with the same 4x4 pin mesh used in the results shown in Table IV. The PARCS core calculations were performed with both diffusion and SP_3 approximations at both 2 and 8 energy groups. SPH factors were not used for radial reflector assemblies with configuration different than the one shown in Table III. The 2-D results are summarized in Table VI. (Note: The results for "No SPH" are the same as results shown previously in Table IV).

Table VI. PARCS 2-D VENUS-2 results with SPH factors.

	Group	Angle	Core k_{eff}	Pin Type %RMS			
				UO_2 3.3	UO_2 4.0	MOX	All
No SPH*	2	Diffusion	0.99727	3.50	1.71	5.96	4.22
		SP_3	1.00486	3.24	2.00	6.09	4.27
	8	Diffusion	0.99360	1.78	1.39	3.22	2.33
		SP_3	1.00284	1.80	1.55	3.27	2.39
SPH*	2	Diffusion	0.99779	4.35	3.32	3.14	3.61
		SP_3	1.00017	4.55	3.37	3.43	3.91
	8	Diffusion	0.99501	1.97	1.97	6.18	4.07
		SP_3	0.99783	1.53	2.24	6.21	4.07

*4x4 mesh per pin

As indicated in Table VI, the application of the SPH factors improved the accuracy of the eigenvalue prediction and made the eigenvalue less sensitive to space, energy and angular discretization. However, the pin power prediction does not improve, and as shown in Figure 5 is much worse along the core / reflector boundary (bottom of the figure). This appears to be attributable to the questionable validity of single assembly SPH factors for the VENUS-2 core where assembly interface effects are particularly important.

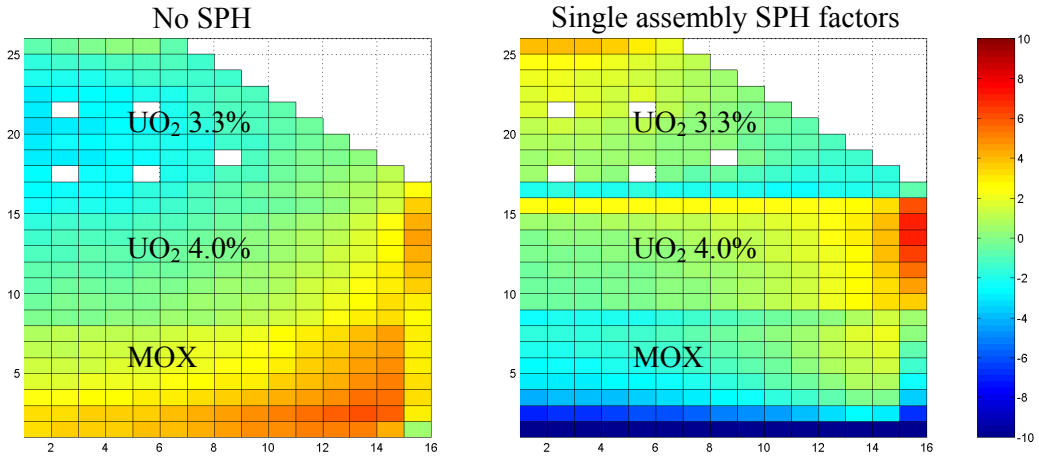

Figure 5. Pin power relative percent error for 8 group, SP_3 solution.

In an attempt to improve the results, another set of PARCS calculations was performed which used HELIOS single assembly calculations in the core interior, but used "two-assembly" HELIOS calculations for the core / reflector interface, as shown in Table III. The results are summarized in Table VII.

Table VII. PARCS 2-D VENUS-2 results with SPH factors from fuel/reflector colorset.

	Group	Angle	Core k_{eff}	Pin Type %RMS			
				UO_2 3.3	UO_2 4.0	MOX	All
No SPH*	2	Diffusion	0.99727	3.50	1.71	5.96	4.22
		SP_3	1.00486	3.24	2.00	6.09	4.27
	8	Diffusion	0.99360	1.78	1.39	3.22	2.33
		SP_3	1.00284	1.80	1.55	3.27	2.39
SPH*	2	Diffusion	0.99326	6.06	5.46	2.50	4.82
		SP_3	0.99507	6.13	5.71	2.58	4.95
	8	Diffusion	0.99666	5.47	5.05	3.31	4.64
		SP_3	0.99745	3.72	3.33	2.71	3.25

*4x4 mesh per pin

A comparison of the results in Table VI and Table VII indicates that the pin power prediction improved in the MOX region, however, the pin error became worse in the UOX region. As indicated in Figure 6, explicit modeling of the fuel / reflector in generating SPH factors reduces the pin errors at the core boundary, but increases the error at the UO_2 3.3% - UO_2 4.0% assembly interface. This exposes the weakness of the SPH factors generated from single assembly calculations and indicates the importance of using "color-set" calculations to generate SPH factors. However, color-set calculations for practical Light Water Reactor models may be too cumbersome for core analysis.

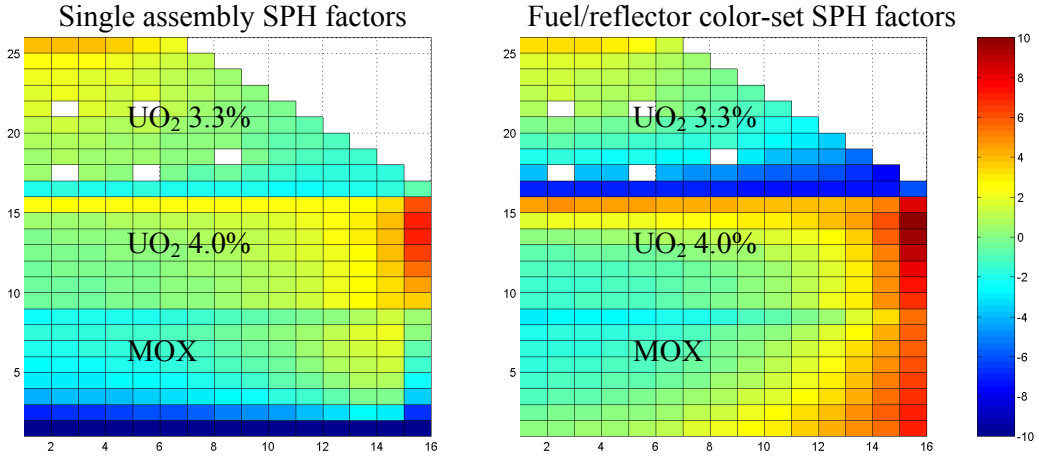

Figure 6. Pin power relative percent error for 8 group, SP_3 solution.

CONCLUSIONS

The focus of the work reported here was the benchmarking of the recently developed multigroup, fine mesh SP_3 methods in PARCS using the VENUS-2 critical experiments. Both the two- and three-dimensional versions of the benchmark were analyzed with PARCS using group constants generated with the HELIOS lattice physics code. The 2-D VENUS-2 benchmark was performed with a specified axial buckling and PARCS results were compared to a full core transport solution generated with HELIOS. Reasonably good agreement was observed between the PARCS 8 group, fine mesh SP_3 solution and the HELIOS solution, both for the core eigenvalue and for the pin power predictions. The 3-D VENUS-2 benchmark is still a "blind" benchmark and assembly and axial power distributions from PARCS results were reported. The PARCS core calculation was also performed using a conventional 2 group nodal calculation with pin power reconstruction using the ANM kernel in PARCS. The errors in the lower order were much larger than those observed with the higher order PARCS solution, particularly when the number of energy groups was reduced from 8 to 2. An initial investigation was also performed using SPH factors generated from single assembly HELIOS calculations to recover errors introduced by various lower order approximations. While the error in the eigenvalue prediction was reduced with SPH factors in PARCS, the pin power prediction was not improved. The apparent reason for the failure of SPH theory as applied here is the questionable validity of single assembly SPH factors for the VENUS-2 core where assembly interface effects are particularly important.

ACKNOWLEDGEMENTS

This work was supported by the U.S. NRC and the Department of Education GAANN program.

REFERENCES

1. C. H. Lee and T. J. Downar, "Application of a Two-Level Acceleration Method to the Pin-by-Pin Multigroup SP_3 Approximation," *Trans. Am. Nucl. Soc.*, **85**, 243 (2001).
2. T. J. Downar, et. al., "PARCS: Purdue Advanced Reactor Core Simulator," *International Conference on the New Frontiers of Nuclear Technology: Reactor Physics, Safety and High-Performance Computing*, PHYSOR 2002, Seoul, Korea, October 7-10, 2002.
3. B. C. Na, "Benchmark on the VENUS-2 MOX Core Measurements," OECD/NEA report, NEA/NSC/DOC(2000)7.
4. B. C. Na, "Blind Benchmark on the 3-D VENUS-2 MOX Core Measurements," OECD/NEA report, NEA/SEN/NSC/WPPR(2001)1.
5. F. D. Giust, R. J. J. Stamm'ler, A. A. Ferri, "HELIOS 1.7 User Guide and Manual," Studsvik Scandpower, 2001.
6. K. B. Lee, "Verification of Equivalent Radial Reflector Cross Sections by Using CASMO-3 for PWR Core Design," CASMO User's Meeting, Feb. 22-24, 1995.
7. M. A. Smith, et. al. "Whole-Core Neutron Transport Calculations Without Fuel-Coolant Homogenization," *International Topical Meeting on Advances in Reactor Physics and Mathematics and Computation into the Next Millennium*, PHYSOR 2000, Pittsburgh, Pennsylvania, USA, May 7-12, 2000.
8. A. Hebert, "A Consistent Technique for the Pin-by-Pin Homogenization of a Pressurized Water Reactor Assembly," *Nucl. Sci. Eng.*, **113**, 227 (1993).